

Linear Magnetoelectric Effect by Orbital Magnetism

A. Scaramucci,^{1,*} E. Bousquet,^{1,2} M. Fechner,¹ M. Mostovoy,³ and N. A. Spaldin¹

¹Materials Theory, ETH Zurich, Wolfgang-Pauli-Strasse 27, CH-8093 Zurich, Switzerland

²Physique Théorique des Matériaux, Université de Liège, B-4000 Sart Tilman, Belgium

³Zernike Institute for Advanced Materials, University of Groningen, Nijenborgh 4, 9747AG Groningen, The Netherlands

(Received 2 August 2012; published 8 November 2012)

We use symmetry analysis and first-principles calculations to show that the linear magnetoelectric effect can originate from the response of orbital magnetic moments to the polar distortions induced by an applied electric field. Using LiFePO₄ as a model compound we show that spin-orbit coupling partially lifts the quenching of the 3*d* orbitals and causes small orbital magnetic moments ($\mu_{(L)} \approx 0.3\mu_B$) parallel to the spins of the Fe²⁺ ions. An applied electric field **E** modifies the size of these orbital magnetic moments inducing a net magnetization linear in **E**.

DOI: 10.1103/PhysRevLett.109.197203

PACS numbers: 75.85.+t, 71.15.Mb, 75.47.Lx

The last decade has seen increasing interest in the study of coupling between electric polarization and intrinsic magnetic moments in materials [1]. Such magnetoelectric coupling manifests in numerous macroscopic phenomena such as type-II multiferroism [2] where the onset of magnetic order induces a spontaneous polarization, and linear magnetolectricity, where an applied electric field **E** (magnetic field, **H**) induces a magnetization $M_j = \alpha_{ij}E_i$ (polarization, $P_i = \alpha_{ij}H_j$). These two phenomena are believed to share closely related microscopic mechanisms.

First-principles computations have been particularly informative in resolving quantitatively the microscopic contributions to the magnetolectric response [3–5]. The first study [3] extracted the “ionic spin” contribution to α , by calculating the change in spin canting caused by freezing in an **E**-induced polar distortion of the ions [6] without additionally explicitly coupling **E** to the electrons. Subsequently, the methodology to calculate the “electronic spin” component was implemented through calculating the electric polarization induced by an applied Zeeman **H** field coupled only to the spin component of the magnetization [4]. Here, the electronic spin response is obtained by “clamping” the ions during the calculation; relaxing the ionic positions in response to the **H** field yields the sum of the ionic and electronic spin components. (Note that, if the lattice constant is also allowed to relax—which was not done in Ref. [4]—an additional strain-mediated ionic response can be extracted). Interestingly, this study showed that the ionic and electronic contributions to α can have similar magnitudes.

These spin-based contributions to α have been shown to capture much of the experimental response. For the case when the magnetic field is applied perpendicular to the spins in a collinear antiferromagnet, the magnetolectric coupling, α_{\perp} , is relativistic in origin, resulting, e.g., from the *E* dependence of the antisymmetric Dzyaloshinskii-Moriya exchange [5,7]. The calculated zero Kelvin polarizations are consistent with experimental values [3], and

the temperature evolution of α_{\perp} follows that of the antiferromagnetic order parameter [7]. The behavior of α_{\parallel} —with the magnetic field applied parallel to the spins—is more complicated. Here, the Heisenberg exchange interactions between spins induce an electric polarization at finite temperature which is approximately an order of magnitude larger than that of relativistic origin responsible for α_{\perp} [5]. Responses calculated within this Heisenberg exchange model [5] agree closely with experiment in the region close to T_N [Fig. 1(a)] [8]. One experimental feature is lacking, however: while the Heisenberg exchange predicts $\alpha_{\parallel} \rightarrow 0$ for $T \rightarrow 0$ K, consistent with the vanishing parallel spin susceptibility at zero Kelvin, many magneto-electrics with collinear antiferromagnetism have nonzero α_{\parallel} at zero Kelvin, and instead follow the temperature dependence sketched in Fig. 1(a) (solid line). An obvious

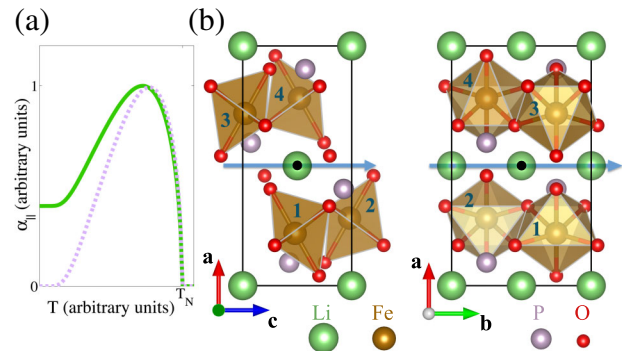


FIG. 1 (color online). (a) Qualitative sketches of the temperature dependence of α_{\parallel} in collinear antiferromagnetic magneto-electrics such as LiFePO₄ (solid line) or Cr₂O₃ (analogous but with negative zero temperature value) and that calculated within a spin-exchange striction mechanism (dashed line). (b) The orthorhombic unit cell of LiFePO₄ contains four Fe²⁺ magnetic cations which are coordinated by distorted oxygen octahedra. The arrows indicate the screw rotation axis parallel to **b** and **c**. The black dot indicates the inversion center.

candidate for the discrepancy is the neglect of orbital contributions [9].

While the neglect of orbital magnetism in the above methods is partially justified by the strong quenching of $3d$ orbital moments which usually occurs in transition metal oxides, spin-orbit coupling, $H_{so} = \lambda \mathbf{L} \cdot \mathbf{S}$, can reduce the quenching, and allow a non-negligible orbital magnetization. This scenario is likely in the collinear antiferromagnets LiFePO_4 and LiCoPO_4 . Both of these compounds have a substantially nonzero α_{\parallel} as $T \rightarrow 0$ and an anomalously large anisotropy of the magnetic g -tensor [10,11].

Few examples, for limited cases and approximations, of calculation of the orbital contribution to the magnetoelectric response exist in the literature. An early study of LiCoPO_4 calculated the “electronic orbital” (clamped ion) contribution analytically by determining the change in the g -factor with electric field using perturbation theory within a single-ion Hamiltonian [12]. While giving a nonzero value for α_{\parallel} at $T = 0$, this method underestimated its magnitude. Recently first-principles finite-electric-field methods were used to calculate the electronic orbital contributions to the trace of the magnetoelectric tensor—the Chern-Simons term—for Cr_2O_3 and BiFeO_3 [13,14]. This contribution was shown to be negligible with respect to the spin contribution in both cases. We emphasize that here we discuss specifically the linear magnetoelectric effect in insulating systems. In metallic systems such as Fe films [15] it has been shown that magnetic anisotropy, and thus orbital moments, may depend significantly on an electric field coupled only to electrons and that this dependency can lead to nonlinear magnetoelectric effects such as the electric field induced flop of the magnetic easy axis in Fe-Au-Fe heterosystems. In this Letter we explore the remaining “ionic orbital” contribution to the magnetoelectric response by calculating the dependence of the local, on-site orbital magnetic moments on polar lattice distortions using density functional theory [16]. Using LiFePO_4 as a model compound, we show that this ionic orbital contribution to α is unexpectedly large and can explain the anomalous low-temperature behavior observed in certain components of α that were previously not understood.

LiFePO_4 is orthorhombic ($Pnma$) and its unit cell [Fig. 1(b)] contains four magnetic sublattices occupied by Fe^{2+} ($S = 2$) ions. Each magnetic ion is surrounded by strongly distorted polar oxygen octahedra with local C_s symmetry. At temperatures below $T_N \approx 50$ K the Fe^{2+} magnetic moments order in the antiferromagnetic collinear structure with order parameter $\mathbf{G} = \mathbf{m}_1 - \mathbf{m}_2 + \mathbf{m}_3 - \mathbf{m}_4$ where \mathbf{m}_i is the magnetization of the i th sublattice. The spin orientation in the antiferromagnetic state remains slightly controversial. Early elastic neutron scattering and x-ray diffraction data suggested that the magnetic moments are oriented along the b direction [17,18]. However, recent

neutron scattering measurements [19] suggest a magnetic structure in which \mathbf{G} is slightly rotated from \mathbf{b} . In this Letter, we study only those components allowed with $\mathbf{G} \parallel \mathbf{b}$; $G^a \neq 0$ or $G^c \neq 0$ would give rise to additional nonzero components of the magnetoelectric tensor (see the Supplemental Material [20]) that have not yet been reported. The magnetic space group of this antiferromagnetic state is $Pnma'$ (magnetic point group mmm') [17,21].

The onset of the antiferromagnetic order breaks inversion symmetry and allows for linear magnetoelectric couplings in the free energy

$$\Phi_{\parallel} = \lambda_{\parallel} G^b E^a H^b \quad \text{and} \quad \Phi_{\perp} = \lambda_{\perp} G^b E^b H^a, \quad (1)$$

where $\lambda_i = \alpha_i/G^b$ and the subscript denotes a magnetic field longitudinal or transverse to the collinear magnetic moments.

α_{\parallel} follows the typical form discussed previously and sketched in Fig. 1(a): Decreasing the temperature from T_N , α_{\parallel} rapidly increases and reaches a maximum at $T_{\max} \approx 45$ K. Below T_{\max} , α_{\parallel} decreases until 20 K at which it becomes almost temperature independent with a value of ~ 2 ps/m [22], not approaching zero as $T \rightarrow 0$ K. α_{\perp} has the simpler temperature dependence mentioned earlier, increasing with decreasing temperature below T_N to reach a roughly constant value below 25 K (4 ps/m) [23].

We focus on the microscopic couplings which can induce α_{\parallel} . Phenomenologically, exchange-striction couplings between electric polarization and spins are allowed by symmetry and give rise to the term $P^a \propto (\mathbf{m}_1 \cdot \mathbf{m}_3 - \mathbf{m}_2 \cdot \mathbf{m}_4)$ (Table I). This coupling results in a temperature behavior of α_{\parallel} similar to that discussed previously for Cr_2O_3 [5] as shown in Fig. 1(a). We note that the local symmetry C_s of the crystal field around each Fe^{2+} ion has only one-dimensional irreducible representations giving nondegenerate d orbitals. When the orbital moments are fully quenched the magnetic moment at the i th site is proportional to the spin $\mathbf{m}_i = 2\mu_B \mathbf{S}_i$. Since at $T = 0$ the spins in a uniaxial antiferromagnet are not modified by \mathbf{H}_{\parallel} weaker than the magnetic field necessary to flop the spins.

TABLE I. Transformation of the four magnetic sublattices (second to fifth column) under the three generators of the space group (modulo a primitive translation) of LiFePO_4 : inversion I , twofold screw rotations around the \mathbf{c} axis 2_c , and \mathbf{b} axis 2_b . Columns six to eight show the transformation of three components of Λ_i . Here the subscripts refer to the change of magnetic sublattice, e.g., $2_c(\Lambda_3^{cb}) = -\Lambda_{2_c(3)}^{cb} = -\Lambda_4^{cb}$. The last three columns show the transformations of \mathbf{E} .

	1	2	3	4	Λ_i^{ab}	Λ_i^{bb}	Λ_i^{cb}	E^a	E^b	E^c
I	4	3	2	1	$\Lambda_{I(i)}^{ab}$	$\Lambda_{I(i)}^{bb}$	$\Lambda_{I(i)}^{cb}$	$-E^a$	$-E^b$	$-E^c$
2_c	2	1	4	3	$\Lambda_{2_c(i)}^{ab}$	$\Lambda_{2_c(i)}^{bb}$	$-\Lambda_{2_c(i)}^{cb}$	$-E^a$	$-E^b$	E^c
2_b	4	3	2	1	$-\Lambda_{2_b(i)}^{ab}$	$\Lambda_{2_b(i)}^{bb}$	$-\Lambda_{2_b(i)}^{cb}$	$-E^a$	E^b	$-E^c$

The electric polarization generated at $T = 0$ by these couplings in response to \mathbf{H}_{\parallel} is zero.

Next we analyze the orbital contribution to α_{\parallel} . We first discuss the orientation and size of orbital moments in zero applied field. From an atomistic perspective, when $H_{\text{so}} = \lambda \mathbf{L} \cdot \mathbf{S}$ is considered the orbital moments are partially unquenched and the magnetic moment at site i is

$$m_i^{\mu} = \mu_B(2S_i^{\mu} + L_i^{\mu}) = \mu_B g_i^{\mu\nu} S_i^{\nu}, \quad (2)$$

where \mathbf{L}_i and $g_i^{\mu\nu}$ are, respectively, the orbital momentum operator and the gyromagnetic tensor at site i , $\mu, \nu = a, b, c$, and summation over repeated indexes is implied. For an ion with a nondegenerate ground state, first-order corrections in λ lead to $g_{\mu\nu} = (2 - \lambda \Lambda_i^{\mu\nu})$ where $\Lambda_i^{\mu\nu} = \sum_n \frac{\langle \psi_0 | L^{\mu} | \psi_n \rangle \langle \psi_n | L^{\nu} | \psi_0 \rangle}{\epsilon_n - \epsilon_0}$. Here ψ_0 is the ground state wave function and ϵ_n and ψ_n are, respectively, the energy and the wave function of the n th excited state of the Fe^{2+} ion at site i . Since the magnetic moments are parallel to \mathbf{b} we consider the components $\Lambda_i^{\mu b}$. The transformations of these components under the generators of the crystallographic space group (modulo primitive translations) [24] are listed in Table I, where we see that $\Lambda_i^{ab} = \Lambda_i^{cb} = 0$ and $\Lambda_i^{bb} \equiv \Lambda^{bb}$ at every magnetic sublattice (see the Supplemental Material [20]).

The mean values of the orbital parts of the magnetic moments induced by the antiferromagnetic ordering are $\mu_{(L)i}^b = -\lambda \Lambda_i^{bb} \langle S_i^b \rangle$ where, for d^6 ions, $\lambda < 0$; therefore, the orbital moment is parallel to the spins.

Next we consider the case $E \neq 0$. Electric-field-induced polar lattice distortions modify the crystal field around each Fe^{2+} ion and the energies $\epsilon_n(\mathbf{E})$. Expanding $\Lambda_i^{\mu\nu}$ to first order in \mathbf{E} one obtains $\Lambda_i^{\mu,\nu}(E) = \Lambda_i^{\mu,\nu}(0) + E^{\alpha} \partial_{E^{\alpha}} \Lambda_i^{\mu,\nu}$, where

$$\partial_{E^{\alpha}} \Lambda_i^{\mu\nu} = - \sum_n \frac{\langle \psi_0 | L^{\mu} | \psi_n \rangle \langle \psi_n | L^{\nu} | \psi_0 \rangle}{(\Delta \epsilon_n)^2} \frac{\partial (\Delta \epsilon_n)}{\partial E^{\alpha}} + \xi_{\rho}^{\mu\nu} \quad (3)$$

and $\Delta \epsilon_n = \epsilon_n(\mathbf{E}) - \epsilon_0(\mathbf{E})$. $\xi_{\rho}^{\mu\nu}$ are the remaining terms containing derivatives of wave functions with respect to E^{α} . The transformations of the derivatives $\partial_{E^{\alpha}} \Lambda_i^{\mu b}$ under the space group of LiFePO_4 can be obtained from those of $\Lambda_i^{\mu b}$ and \mathbf{E} (see the Supplemental Material [20]) in Table I. From these transformations we obtain $\partial_{E^a} \Lambda_1^{bb} = \partial_{E^a} \Lambda_3^{bb} = -\partial_{E^a} \Lambda_2^{bb} = -\partial_{E^a} \Lambda_4^{bb} \equiv \partial_{E^a} \Lambda^{bb}$. Therefore, the response of the average orbital-induced magnetic moment to an electric field along \mathbf{a} gives rise to a net magnetization along \mathbf{b}

$$\mu_{(L)}^b = \mu_B \partial_{E^a} \Lambda^{bb} (\langle S_1^b \rangle - \langle S_2^b \rangle + \langle S_3^b \rangle - \langle S_4^b \rangle) E^a \quad (4)$$

that at $T = 0$ gives $\mu_{(L)}^b = 4\mu_B S \partial_{E^a} \Lambda^{bb} E^a$.

To calculate the strength of the linear magnetoelectric coupling arising from this mechanism, we perform first-principles calculations using the Vienna *ab initio* simulation package (VASP) [25]. We use a plane-wave basis set for the expansion of the electronic valence wave function and projector augmented wave [26] potentials for the treatment of core electrons. The exchange-correlation potential is described within the local-spin-density approximation plus a rotationally invariant Hubbard- U (LSDA + U) with a U value of 5 eV, and J values between 0 and 1 eV. Calculations are performed keeping lattice parameters fixed at the experimental unit cell volume of 291 \AA^3 [18]. Therefore, we do not consider strain-mediated contributions. We first relax the structure in the absence of spin-orbit coupling and then we include spin-orbit coupling to calculate the orbital magnetic moment. We obtain an orbital moment $\mu_{(L)} = 0.306 \mu_B$ parallel to the spins, with $J = 1$ eV. Note that the magnitude of the magnetic moment depends on J and on the PAW sphere radius as discussed in the Supplemental Material [20].

To calculate the ionic orbital response—the change in orbital magnetic moments when the ions are displaced by E —we adapt the framework introduced in Ref. [3] for the ionic spin response. As in Ref. [3], we shift the equilibrium positions \mathbf{r}_i of the ions by $\Delta r_i^{\mu} = E^{\rho} \sum_{\nu j} \phi_{\mu i, \nu j}^{-1} Z_{j, \rho \nu}^*$ where $\phi_{\mu i, \nu j}^{-1}$ is the inverse of the force constant matrix after the acoustic modes are traced out and $Z_{j, \rho \nu}^*$ are the Born effective charges, both calculated in the absence of spin-orbit coupling. Since we aim to separate the orbital from the spin contribution, we constrain the orientation (but not the magnitude) of the spins to lie along the b direction, which we call the “clamped spin” approximation. After making the Δr_i^{μ} distortions from the equilibrium zero-field positions, we relax the electronic density with spin-orbit coupling included and calculate the resulting orbital magnetic moments.

Figure 2(a) shows the evolution of the calculated net orbital magnetic moment $\mu_{(L)} = \sum_{i=1,4} \mu_{(L),i}$ of one unit cell of LiFePO_4 for an electric field applied along \mathbf{a} with $J = 1$ eV (blue) and $J = 0$ eV (red). (Note that, while the electric field is applied perpendicular to the spins, this corresponds to the parallel component of α , since the magnetoelectric response is off diagonal). We find that at nonzero electric field the orbital moments remain parallel to the spins, and consistent with Eq. (4) their change in size is opposite for odd and even magnetic sublattices giving a net magnetization. The linear fits of the E^a responses of the orbital magnetization at $J = 1$ eV (blue line) and $J = 0$ eV (red line) give $\alpha_{\parallel} = 2.3$ ps/m and $\alpha_{\parallel} = 9.3$ ps/m, respectively. The α_{\parallel} value for $J = 1$ eV is close to the experimental value of $\alpha_{\parallel} \sim 2$ ps/m at $T = 0$ K [21,23]. This J value is consistent with Ref. [27] which showed that $J > 0.6$ eV is needed to obtain the correct magnetic easy axis.

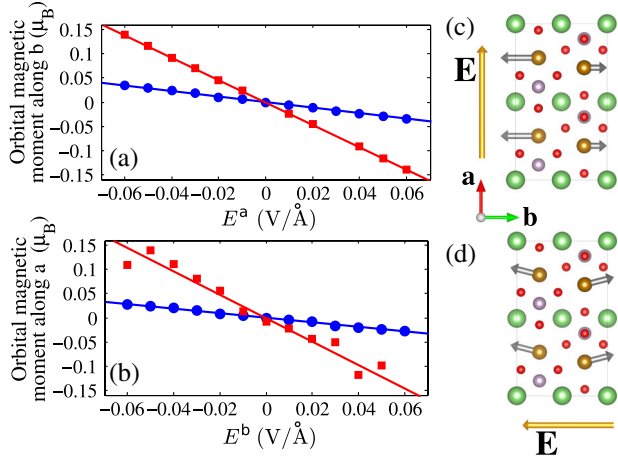


FIG. 2 (color online). Calculated electric-field dependence of the net orbital magnetic moment per unit cell. (a) $\mathbf{E} \parallel \mathbf{a}$ results in an orbital magnetization along \mathbf{b} (α_{\parallel}). (b) $\mathbf{E} \parallel \mathbf{b}$ produces a net orbital magnetic moment along \mathbf{a} (α_{\perp}). Blue dots and red squares are calculated with $J = 1$ eV and $J = 0$ eV, respectively; the lines are linear fits to the calculated values. The cartoons on the right panels show the size and orientation of the orbital magnetic moments (gray arrows) of Fe^{2+} (brown spheres with attached arrows) when the electric field is applied along \mathbf{a} (c) and \mathbf{b} (d).

To summarize this section, we find that the calculated zero Kelvin ionic orbital contribution to α_{\parallel} has a value which is consistent with the measured value of α_{\parallel} . We suggest, therefore, that the previous discrepancy between the measured zero Kelvin magnetoelectric response and the calculated spin-only response can be explained by this contribution. At nonzero temperatures, contributions to α_{\parallel} that are inactive in the absence of thermal fluctuations have to be taken into account. These terms comprise the electric field dependence of single-ion anisotropy, which has the same nature as the orbital magnetic moment, as well as the Heisenberg interactions mentioned earlier.

Finally, we investigate the ionic orbital contribution to α_{\perp} by calculating the effect of an electric field applied along \mathbf{b} . While the spin-only contribution was not inconsistent with experiment in this case, contributions to α_{\perp} from the electric field dependence of $\mu_{(L)i}$ have not been previously investigated and might also play a role. First we use symmetry arguments to find the constraints on $\partial_{E^b} \Lambda_i^{\mu\nu}$. From Table I we find $\partial_{E^b} \Lambda_1^{ab} = \partial_{E^b} \Lambda_3^{ab} = -\partial_{E^b} \Lambda_2^{ab} = -\partial_{E^b} \Lambda_4^{ab} \equiv \partial_{E^b} \Lambda^{ab}$, $\partial_{E^b} \Lambda_1^{cb} = \partial_{E^b} \Lambda_2^{cb} = -\partial_{E^b} \Lambda_3^{cb} = -\partial_{E^b} \Lambda_4^{cb} \equiv \partial_{E^b} \Lambda^{cb}$ and $\partial_{E^b} \Lambda_i^{bb} = 0$. We note that the transformation properties of $\partial_{E^b} \Lambda_i^{ab}$ are identical to those of $\partial_{E^a} \Lambda_i^{bb}$. This allows for a linear dependence of the orbital magnetization along \mathbf{a} when the electric field is applied along \mathbf{b} : $\mu_a = 4\mu_B E^b \partial_{E^b} \Lambda^{ab} |\langle S^b \rangle|$ where $|\langle S^b \rangle|$ is the absolute value of the average spin component along \mathbf{b} . In contrast, the spin ordering of LiFePO_4 combined with the transformation properties of $\partial_{E^b} \Lambda_i^{cb}$ yields opposite changes in the orbital moment along \mathbf{c} under the applied

E^b field for sublattices 1, 4 compared with 2, 3 and zero net moment in this direction. To obtain the size of the ionic orbital contribution to α_{\perp} we perform *ab initio* calculations using the same method discussed for α_{\parallel} but with \mathbf{E} applied along \mathbf{b} . The resulting calculated values of net orbital moment are shown in Fig. 2(b) as a function of E^b . Here blue and red points show the results for, respectively, $J = 1$ eV and $J = 0$ eV. Even when the spins are constrained parallel to the \mathbf{b} axis, the applied E^b induces a canting of the orbital magnetic moments from the b direction. In agreement with the constraints found for $\partial_{E^b} \Lambda_i^{ab}$ the resulting canting is uniform along the \mathbf{a} axis for all magnetic sublattices giving rise to a net magnetization linear in E^b . Furthermore, as predicted using the transformations of $\partial_{E^b} \Lambda_i^{cb}$ for finite E_b we observe a tiny staggered canting of the orbital moment along c which gives rise to zero net magnetization. The solid lines in Fig. 2(b) are linear interpolations of the calculated values and give linear magnetoelectric responses of 1.9 ps/m and 9.7 ps/m for $J = 1$ eV and $J = 0$, respectively. To these values, which contain only the ionic orbital magnetoelectric effect, one should add the spin-only contribution to α_{\perp} , which in contrast to the case of α_{\parallel} does not vanish at $T = 0$. These include the rotation of easy axis anisotropy, which shares the same origin as the canting of the orbital magnetic moment, as well as the Dzyaloshinskii-Moriya interaction. Using the approach described in Ref. [4], which includes these contributions but not the orbital part, we obtain $\alpha_{\perp} = 2.6$ ps/m with sign opposite to the orbital one for $J = 1$ eV. Importantly, these considerations can also be used to describe the resonant excitation of waves of oscillating magnetization $M \parallel \mathbf{a}$ with an oscillating electric field of a light wave $E \parallel \mathbf{b}$, resulting in the so-called “electromagnon” peaks in optical absorption [28]. Thus the coupling between the orbital magnetic moment and the electric field gives rise to both static and dynamic magnetoelectric effects.

In summary, we have shown that a linear magnetoelectric effect can arise from the dependence of orbital magnetic moments on the polar distortions induced by an applied electric field, the so-called “ionic orbital” contribution to the magnetoelectric response. We presented a symmetry analysis to determine the components of $\alpha_{\mu\nu}$ for which this effect exists, and a methodology with which to calculate *ab initio* those components at $T = 0$. We applied the methodology to LiFePO_4 and resolved the previous discrepancy between calculations of the spin-only contributions and experiment for α_{\parallel} . Our results show that the orbital contributions to the magnetoelectric response can be comparable in size to the spin contributions of either relativistic or exchange-striction origin in $3d$ transition metal compounds. As suggested by Eq. (4), the temperature dependence of the magnetoelectric effect caused by orbital magnetism coincides with that of the order parameter which, added to the temperature dependence of the response originating from striction, gives qualitative

agreement for various collinear antiferromagnets such as Cr_2O_3 [29], LiCoPO_4 [30], and TbPO_4 [31].

Furthermore, the strength of such coupling depends on the spin-orbit interaction, energy gaps between ground and excited states for which $\langle \psi_0 | L^\mu | \psi_n \rangle \neq 0$, and the dependence of these states on polar distortions. This suggests that large magnetoelectric effects from orbital moments correlate with the enhanced anisotropic g -tensor and the anisotropy of the magnetic susceptibility in the paramagnetic state. In particular, a large orbital magnetoelectric response might be found in compounds with small electronic gap, containing magnetic ions with large spin-orbit coupling and with low symmetry polar oxygen coordination.

This work was supported by ETH Zürich and by the European Research Council Advanced Grants program under the FP7, Grant No. 291151. E. B. thanks FRS-FNRS Belgium for support.

*andrea.scaramucci@mat.ethz.ch

- [1] M. Fiebig, *J. Phys. D* **38**, R123 (2005).
- [2] D. Khomskii, *Physics* **2**, 20 (2009).
- [3] J. Íñiguez, *Phys. Rev. Lett.* **101**, 117201 (2008).
- [4] E. Bousquet, N. A. Spaldin, and K. T. Delaney, *Phys. Rev. Lett.* **106**, 107202 (2011).
- [5] M. Mostovoy, A. Scaramucci, N. A. Spaldin, and K. T. Delaney, *Phys. Rev. Lett.* **105**, 087202 (2010).
- [6] Note that, while we use the term “ionic spin,” this contribution includes couplings such as the Dzyaloshinskii-Moriya interaction and the electric field dependence of magnetocrystalline anisotropy, both of which are mediated by spin-orbit interaction, in addition to spin-only contributions from exchange striction.
- [7] R. Hornreich and S. Shtrikman, *Phys. Rev.* **161**, 506 (1967).
- [8] Here, in contrast to Ref. [5], we consider mean field theory for a quantum Heisenberg model.
- [9] G. T. Rado, *Phys. Rev.* **128**, 2546 (1962).
- [10] J. Creer and G. Troup, *Phys. Lett. A* **32**, 439 (1970).
- [11] G. Liang, K. Park, J. Li, R. E. Benson, D. Vaknin, J. T. Markert, and M. C. Croft, *Phys. Rev. B* **77**, 064414 (2008).
- [12] I. Kornev, J.-P. Rivera, S. Gentil, A. Jansen, M. Bichurin, H. Schmid, and P. Wyder, *Physica (Amsterdam)* **271B**, 304 (1999).
- [13] S. Coh, D. Vanderbilt, A. Malashevich, and I. Souza, *Phys. Rev. B* **83**, 085108 (2011).
- [14] A. Malashevich, I. Souza, S. Coh, and D. Vanderbilt, *New J. Phys.* **12**, 053032 (2010).
- [15] S. Subkow and M. Fähnle, *Phys. Rev. B* **84**, 054443 (2011).
- [16] A. Malashevich, S. Coh, I. Souza, and D. Vanderbilt, *Phys. Rev. B* **86**, 094430 (2012).
- [17] R. P. Santoro and R. E. Newnham, *Acta Crystallogr.* **22**, 344 (1967).
- [18] V. A. Streltsov, E. L. Belokoneva, V. G. Tsirelson, and N. K. Hansen, *Acta Crystallogr. Sect. B* **49**, 147 (1993).
- [19] J. Li, V. O. Garlea, J. L. Zarestky, and D. Vaknin, *Phys. Rev. B* **73**, 024410 (2006).
- [20] See Supplemental Material at <http://link.aps.org/supplemental/10.1103/PhysRevLett.109.197203> for the effect of small rotation of \mathbf{G} away from \mathbf{b} , a more detailed symmetry analysis, convergence of orbital magnetic moments and additional technical details.
- [21] A. Borovik-Romanov and H. Grimmer, in *International Tables for Crystallography* edited by A. Authier, H. Fuess, T. Hahn, H. Wondratschek, U. Müller, U. Shmueli, E. Prince, A. Authier, V. Kopsk, D. Litvin, M. Rossmann, E. Arnold, S. Hall, and B. McMahon (Springer, Netherlands, 2003), Volume D: Physical Properties of Crystals, pp. 105–149.
- [22] Since the $\alpha_{\parallel}(T)$ curve in Ref. [23] is in arbitrary units, we set its maximum to the value of $\alpha_{\parallel}^{\text{max}} = 10^{-4}$ (Gaussian units) ≈ 4.2 ps/m from Ref. [21] in order to estimate $\alpha_{\parallel}(T = 0)$.
- [23] M. Mercier, P. Bauer, and B. Fouilleux, *C. R. Acad. Sc. Paris* **267**, 1345 (1968).
- [24] As terms in the Hamiltonian and free energy expansion have to be invariant under the transformation of the high-symmetry state (paramagnetic state) we study transformations of $\Lambda_i^{\mu\nu}$ and $\partial_{E^\alpha} \Lambda_i^{\mu\nu}$ under the crystallographic space group.
- [25] G. Kresse and J. Furthmüller, *Phys. Rev. B* **54**, 11169 (1996).
- [26] G. Kresse and D. Joubert, *Phys. Rev. B* **59**, 1758 (1999).
- [27] E. Bousquet and N. Spaldin, *Phys. Rev. B* **82**, 220402 (2010).
- [28] A. Pimenov, A. A. Mukhin, V. Y. Ivanov, V. D. Travkin, A. M. Balbashov, and A. Loidl, *Nat. Phys.* **2**, 97 (2006).
- [29] E. Sirtori, K. Tasaki, and A. Kita, *J. Appl. Phys.* **50**, 7748 (1979).
- [30] J.-P. Rivera, *Ferroelectrics* **161**, 147 (1994).
- [31] G. T. Rado, J. M. Ferrari, and W. G. Maisch, *Phys. Rev. B* **29**, 4041 (1984).